PERGAMON

Vision Research 39 (1999) 4309–4323

Vision Research

www.elsevier.com/locate/visres

A new approach to the study of ocular chromatic aberrations

Susana Marcos [a,*], Stephen A. Burns [b], Esther Moreno-Barriusop [b], Rafael Navarro [b]

[a] *Schepens Eye Research Institute, 20 Staniford Street, Boston, MA 02114, USA*
[b] *Instituto de Óptica, 'Daza de Valdés', Consejo Superior de Investigaciones Científicas, Serrano 121, Madrid 28006, Spain*

Received 11 March 1999; received in revised form 16 June 1999

Abstract

We measured the ocular wavefront aberration at six different visible wavelengths (between 450 and 650 nm) in three subjects, using a spatially resolved refractometer. In this technique, the angular deviation of light rays entering the pupil at different locations is measured with respect to a target viewed through a centered pupil. Fits of the data at each wavelength to Zernike polynomials were used to estimate the change of defocus with wavelength (longitudinal chromatic aberration, LCA) and the wavelength-dependence of the ocular aberrations. Measured LCA was in good agreement with the literature. In most cases the wavefront aberration increased slightly with wavelength. The angular deviations from the reference stimulus measured using a magenta filter allowed us to estimate the achromatic axis and both optical and perceived transverse chromatic aberration (TCA), (including the effect of aberrations and Stiles–Crawford effect). The amount of TCA varied markedly across subjects, and between eyes of the same subject. Finally, we used the results from these experiments to compute the image quality of the eye in polychromatic light.

Keywords: Wavefront aberration; Transverse and longitudinal chromatic aberration; Achromatic axis; Stiles–Crawford effect; Optical quality of the human eye; Polychromatic light

1. Introduction

Chromatic aberrations arise from the dispersion in the ocular refracting elements. We can distinguish two general types of chromatic aberrations: (1) chromatic variations in the paraxial image-forming properties of the optical system; and (2) wavelength dependence of the monochromatic aberrations.

Typically, only the first type of chromatic aberration has been characterized in the human eye, classified in two components: the longitudinal or axial chromatic aberration (LCA), and the transverse or lateral chromatic aberration (TCA). Longitudinal chromatic aberration is the dependence of the refractive power of the eye with wavelength (the refractive index, and hence the ocular refractive power is higher for short wavelengths), and it has been measured extensively, both subjectively (Wald & Griffin, 1947; Ivanoff, 1953; Bedford & Wyszecki, 1957; Jenkins, 1963; Howarth & Bradley, 1986), and objectively by Charman and Jennings (1976a) and Rynders, Navarro and Losada (1998), who used retinoscopic methods. LCA has been found to be about two diopters (D) across the visible spectrum, with some differences across studies. This value is consistent with theoretical computations based on the dispersion of the ocular media (Emsley, 1952; Thibos, Bradley, Still, Zhang, & Howarth, 1990). The second manifestation of chromatic aberration traditionally described is the transverse chromatic aberration (TCA), which is the difference in the angular displacement of the retinal image for different wavelengths. TCA is typically measured by vernier alignment techniques, using bichromatic (red and blue) targets (Hartridge, 1947; Kishto, 1965; Ogboso & Bedell, 1987; Simonet & Campbell, 1990; Thibos et al., 1990). The effect of TCA is particularly important for decentered pupils (Thibos, Bradley & Zhang, 1991; Artal, Marcos, Iglesias, & Green, 1996) and increases with retinal eccentricity (Ogboso & Bedell, 1987; Thibos, 1987). Since the optical system of the eye is generally not centered, the TCA is non-zero on the visual axis. Whereas the LCA does not show a great intersubject variability, reports of the TCA from different studies are significantly different in

* Corresponding author. Fax: +1-617-912-0111.
E-mail address: susana@vision.eri.harvard.edu (S. Marcos)

0042-6989/99/$ - see front matter
PII: S0042-6989(99)00145-5

both amount and direction. Part of the variability could be accounted for by individual differences in the position of the fovea with respect to the optical axis (Le Grand, 1956), deviations in pupil centration (Walsh, 1988), and different degrees of misalignment of the optical components of the eye. Differences may also arise from differences in the measurement conditions (pupil size, luminance, etc.). Whereas some studies are performed using a centered pinhole pupil or Maxwellian view — and thus measured the optical TCA — (Simonet & Campbell, 1990; Thibos et al., 1990) others use normal view (Hartridge, 1947; Kishto, 1965; Ogboso & Bedell, 1987). The latter measurement of TCA is affected by aberrations and the Stiles–Crawford effect (Vos, 1960; Ye, Bradley, Thibos & Zhang, 1992; Rynders, 1994) and therefore it is called perceived TCA.

Although LCA and TCA are the principal manifestations of chromatic aberration, the monochromatic aberrations should also change with wavelength. The monochromatic aberrations depend on both the geometry of the refracting surfaces and elements, as well as on the indices of refraction of the media, which are functions of wavelength. Since the optical aberrations are small compared to the nominal refractive power of the eye (60 D), the differences in the ocular aberrations across the visible spectrum are expected to be much smaller than the equivalent LCA of 2 D. In recent years, there has been an increased interest in the study of the aberrations of the human eye, and a number of techniques to estimate the wavefront aberration of the human eye have been developed (Howland & Howland, 1977; Webb, Penney & Thompson, 1992; Liang, Grimm, Goetz & Bille, 1994; Navarro & Losada, 1997). These techniques typically use monochromatic light, allowing only the estimation of monochromatic aberrations. There have been attempts to characterize the optical image quality in polychromatic light. Charman and Jennings (1976b) found important differences in the optical image quality across wavelengths measured using a double-pass technique, which they attributed to changes in intraocular scattering and signal-to-noise ratio of the photodetector. Marcos, Moreno & Navarro (1999) study on the depth of field of the human eye at different visible wavelengths suggests little variation of the aberrations with wavelength, and other studies have assumed no difference with wavelength other than defocus induced by LCA (Van Meeteren, 1974; Atchinson, Woods & Bradley, 1998).

This study presents, for the first time to our knowledge, direct quantitative measurements of the change of the monochromatic aberrations across the visible spectrum, using a spatially resolved refractometer (Webb et al., 1992; He, Marcos, Webb & Burns, 1998a). We obtained estimates of the wavefront aberration, described as an expansion of Zernike polynomials, for a series of wavelengths. This allowed us to directly measure the overall optical image quality at each wavelength and by extension for polychromatic light. In addition, the same type of data allowed us to estimate the traditional chromatic aberrations (LCA and TCA) in the same subjects. Unlike most previous approaches based on subjective refraction, LCA was estimated directly (from the defocus term in the polynomial expansion of the wavefront aberration). From the same type of data, we computed the achromatic axis (pupil location for which the chromatic parallax is minimum, Thibos et al., 1992; Simonet & Campbell, 1990), as well as the TCA (both horizontal and vertical components). We estimated the differences between optical and perceived TCA, and evaluated directly the effect of both the Stiles–Crawford effect (SCE, available for these subjects from previous measurements) and the aberrations, which often had been hypothesized in the literature to explain differences between measurements of the TCA and the effect of chromostereopsis (Vos, 1960; Sundet, 1972; Simonet & Campbell, 1990; Ye et al., 1992; Rynders, 1994).

2. Methods

2.1. Apparatus

The ocular wavefront aberration was measured using a spatially resolved refractometer. The principle and optical-set up have been described in detail elsewhere (Webb et al., 1992; He et al., 1998a). Since the optics of the eye suffer from aberrations, light from different entry pupil locations does not converge to the retina at a common location, but instead, it is deviated to different retinal locations. The angular deviation of the light at each point in the pupil is a measure of the ray aberration at that point. In this psychophysical technique, we measure the angle that the subject needs to deviate the test spot (which is viewed through a series of pupil locations) to align it to a reference cross viewed through the center of the pupil. The optical system (Fig. 1) consists of three channels: (1) a test channel providing the test spot. The entry pupil location of the test channel is changed in random order by moving a rotating wheel, conjugate to the pupil, with 37 1-mm apertures drilled so that they tile the pupil one at a time, as shown in the inset of Fig. 1. (2) A fixation channel, which projects a back illuminated cross-target slide viewed through a centered pupil (an iris diaphragm, set to 3 mm for the current experiment) and a green filter (Kodak, Wratten 58). The fixation target also contained high frequency information to control the accommodative state (He, Burns & Marcos, 1998b) (3) A pupil monitoring channel, with an IR CCD video camera, which allows constant monitoring of the pupil

size and centration of the optical axis of the system to the geometrical center of the pupil. All channels share a common focusing block, which allows us to correct the refraction of the subject, in a range of 0 to −6 D. We have performed a major change to adapt the existing instrument to the measure of the wavefront aberration at different wavelengths. In the original apparatus (He et al., 1998a), a 543 nm He–Ne laser was used to generate a point source conjugate to the retinal plane. The angle of the beam at the pupil plane (and hence, the retinal location of the spot) was changed by tilting a gimballed mirror by means of a joystick, which the subject moved until he/she perceived it aligned to the center of the reference cross. In the current version of the apparatus, the laser and gimballed mirror have been replaced by an oscilloscope screen optically conjugated to the retinal plane. The subject controls the location of the beam spot on the oscilloscope CRT by changing the X and Y voltages using a joystick. The broad-band (533, 44 nm halfwidth) CRT phosphor, combined with a series of narrow-band interference filters (DitricOptics) allows measurements at different wavelengths. In Experiment 1, we have used the following wavelengths: 450, 490, 530, 570, 620, and 650 nm (10 nm halfwidth). For the middle wavelengths (530 and 570 nm) a neutral density filter was introduced, to maintain the intensity of the test spot approximately constant for all wavelengths. In a separate experiment (Experiment 2) we used a magenta filter, yielding peak wavelengths of 473 (9 nm halfwidth) and 601 nm (13 nm halfwidth) in combination with the oscilloscope spectrum — as calibrated using a spectrophotometer (EG&G/PAR, Model II).

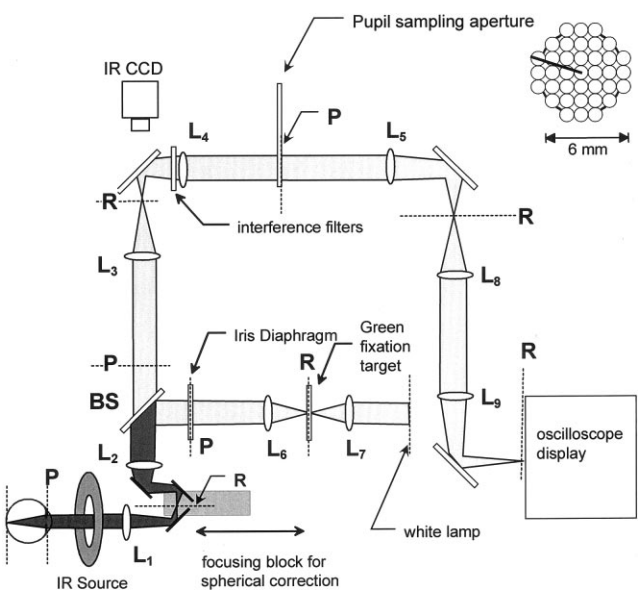

Fig. 1. Schematic diagram of the spatially resolved refractometer apparatus. The test spot is provided by an oscilloscope, and the entry pupil is selected sequentially among the 37 1-mm sample apertures drilled in a spinning wheel. The inset shows the spatial configuration of the sample pupils. The reference channel projects a green cross-target, viewed through a centered iris. The subject's spherical refraction is compensated in these two channels by moving a focusing block. A CCD camera monitors the subject's pupil, illuminated by IR light. P denotes planes optically conjugate to the pupil, and R, planes optically conjugate to the retina. The focal length of lenses L_1–L_6 is 150 mm; L_7 100 mm, L_8 is 50 mm, and L_9 is 350 mm.

2.2. Subjects

We have made measurements on three subjects, two females (EM and SM, ages 25 and 28) and one male (SB, age 48). Their refractive spherical corrections were −0.5 D, −5.5 D and −4.5 D, respectively, and their cylindrical corrections were −0.5 D, −0.25 D and −2.5 D, respectively. Their color vision was normal. Measurements were made under natural pupil and free accommodation to the fixation stimulus. A control experiment was performed with paralyzed accommodation (by means of cyclopentolate 1%).

2.3. Experimental procedure

The test procedure has been described in detail elsewhere (He et al., 1998a). At the start of each experimental session, the experimenter aligns the subject (stabilized my means of a dental impression and head rest) to the apparatus, while he/she monitors the pupil position on a TV screen. The retinal illuminance was kept low to allow pupil sizes of at least 6 mm in diameter[1]. Prior to the measurements, the experimenter corrected the subjective refraction of the subject, using the green fixation target of the reference channel. The same correction in the focusing system was maintained in all runs and sessions for the same subject. Each experimental run consists of a complete set of 39 measurements of the angles required to align the test spot to the center of the reference cross, each corresponding to the 37 entry pupils (in addition to two repeats of the central sample pupil).

2.3.1. Experiment 1

The purpose of this experiment was to determine the variation of the monochromatic aberrations with wave-

[1] For the pupil sampling configuration used in this experiment, a pupil diameter of at least 7.32 mm (3.66 mm radius) would be required for all the light from each aperture to enter the eye. This radius is the length of the segment shown in the inset of Fig. 1. As a result we used this value for coordinate normalization in the Zernike polynomials, and for the rest of calculations. However, the natural pupil was generally between 6 and 7 mm. To determine if this difference between the actual size and the normalization value altered the data, we have computed the error introduced in the Zernike coefficients by considering a 7.32 mm pupil while the actual pupil diameter was 6.25 mm. We found that the error was less than the standard deviation of the measurement.

length and the longitudinal chromatic aberration. All subjects (using their right eye) participated in four experimental sessions with measurements at six different wavelengths (ranging from 450 to 650 nm), and three runs per wavelength. Wavelengths were interleaved to avoid bias in the accommodation during a session. While the wavelength of the test channel was changed by inserting different interference filters, the green filter in the reference channel was kept constant throughout the experiment. Each experimental session (18 runs) lasted typically 90 min.

2.3.2. Experiment 2

The purpose of this experiment was to determine the achromatic axis and the transverse chromatic aberration. Ideally, these functions could be estimated from the set of data in Experiment 1. However, we found that, despite the use of kinematic filter holders, the reproducibility of the filter position from run to run was not sufficiently accurate (we found variations of up to 4.5 arc min). To avoid this problem, we conducted similar experiment to the ones described before, but replaced the separate blue and red filters with a single magenta filter (with peak wavelengths at 473 and 601 nm). This avoided the need to change filters within a session. The subject perceived separate blue and red retinal spots, due to chromatic parallax. Subjects SM and SB (both using left and right eyes) participated in two separate experimental sessions. Each experimental session consisted of six runs: three of them using the blue spot, and the other three, using the red spot. In an additional psychophysical experiment, the subject reported the entry pupil location for which he/she perceived the red and blue spots superimposed.

2.4. Control experiments

Several control experiments were conducted to assess the accuracy of the modified spatially resolved refractometer, as well as the validity of the experimental conditions.

2.4.1. Calibration and accuracy of the spatially resolved refractometer

The spatially resolved refractometer was calibrated as described in He et al. (1998a). We measured the relation between the deviation of the test beam provided by the oscilloscope (i.e. the voltages of X and Y channels in the oscilloscope) and the joystick voltage. All tests of accuracy described in a previous paper, were repeated with the new configuration. Subject SM, who had participated in the previously published measurements, was used for a test of reproducibility between experiments conducted with the previous and the present version of the apparatus (using a 530 nm interference filter). Under similar conditions, the previous and present versions yielded very similar results. The standard deviation of the wavefront root-mean-square (RMS) error and the average standard deviation of Zernike coefficients were 0.0536 and 0.18 μm, respectively, across runs in a single session; 0.080 and 0.19 μm, respectively, across sessions using the same instrument; and 0.086 and 0.22 μm across sessions using the two versions of the instrument. We also confirmed that the apparatus did not suffer from chromatic aberration. We placed a CCD camera with a diffraction-limited achromatic lens in place of the subject's eye. We performed the same experiment, aligning the test spot to the center of the reference cross on a TV monitor. Except for the tilt terms, all Zernike coefficients were not significantly different from zero for all wavelengths used in this experiment: RMS wavefront error was less than 0.20 μm and defocus was less than 0.008 D.

2.4.2. Free accommodation versus cycloplegia

In order to assess the necessity of paralyzing the accommodation, we conducted a control experiment on subject EM (our youngest subject). The experiment was performed in a single session consisting of nine runs: three runs under natural viewing conditions and free accommodation to the fixation stimulus, using a 1 mm pupil in the reference channel; three runs under the same conditions, using a 6 mm pupil in the reference channel; three runs under the effect of cyclopegia, with a 1 mm pupil in the reference channel. The focusing system was not moved throughout the session. The test wavelength was 530 nm. Variability in the data obtained under free-accommodation was similar to the variability under cycloplegia. In particular, the standard deviation of the defocus term (which is the most likely to change under free-accommodation, due to fluctuations in accommodation) was 0.018 μm (or 0.005 D) under free-accommodation and a small pupil, 0.088 μm (or 0.027 D) under free-accommodation and a large pupil, and 0.070 μm (or 0.021 D) under cycloplegia. The mean standard deviation of the rest of the terms in the Zernike expansion was 0.080, 0.085, and 0.085 μm, respectively. We concluded that the use of cyclopentolate did not decrease the variability of the measurements.

2.5. Data analysis

2.5.1. Experiment 1

The data of Experiment 1 were analyzed as described by He et al. (1998a). The data recorded by the computer (tilts necessary to align the test spot to a reference for each entry location) are a discrete measure of the slope of the wavefront aberration at each pupil location. The wavefront aberration is estimated using a least square fit of a Zernike polynomial expansion to the tilts. We fit up to the 7th order of a Zernike

expansion (35 terms), using Mahajan (1994) ordering scheme, which for the purposes of this paper is equivalent to the basis used by Malacara (1992). The set of Zernike coefficients allowed us to estimate, for each wavelength: the continuous wavefront aberration, defocus (which as a function of wavelength provides the chromatic difference of focus or LCA) and classical aberrations such as cylinder or spherical aberration. The root mean square of the Zernike coefficients, appropriately scaled (Noll, 1976), provided a measurement of the optical quality. Other functions that were calculated from the wavefront aberration were the point-spread-function (PSF) and modulation-transfer-function (MTF), from which other parameters describing the optical quality (strehl ratio and volume under the MTF) were computed. We used pupil radii of 3.66 mm in all these computations[1]. In principle, the tilt terms (c_1 and c_2) provide an estimate of the TCA. However, those terms are affected by fitting artifacts when deriving the wavefront from the derivatives of the wavefront aberration, and consequently, they are not reliable.

2.5.2. Experiment 2

The sets of data using the magenta filter were similar to those in Experiment 1 (except for the differences in wavelengths and for the fact that the filter does not need to be exchanged). However, we processed the data differently. We treated the series of tilts as the angular spot diagram in a ray tracing operation. The tilt needed to null the deviation of the retinal spot with respect to the reference viewed through the center of the pupil is equivalent to the angular deviation of the spot from the chief ray. The map of angular deviations for all pupil positions (known as a spot diagram) represents a good approximation to the point-spread-function ignoring diffraction (Navarro, Moreno & Dorronsoro, 1998). The spot diagrams for blue and red illumination are different, due mainly to chromatic difference of focus. Also, the blue spot diagram is laterally displaced with respect to the red spot diagram, due to transverse chromatic aberration (TCA). We estimated the achromatic axis as the entry pupil location that produced minimum chromatic parallax. Optical TCA was estimated as the angular distance between the blue and red retinal spots, for the centered sample aperture. Perceived TCA was estimated as the angular distance between centroids of the blue and red angular spot diagrams, respectively.

3. Results

3.1. Experiment 1

3.1.1. Chromatic difference of focus: longitudinal chromatic aberration

The most noticeable change across wavelengths occurs in the defocus term (Zernike coefficient c_4). Fig. 2 shows the change in the defocus term, expressed in diopters, averaged across runs and subjects. All subjects participating in the experiment were corrected for green illumination, by moving the focusing block to the position for which they best perceived the accommodation target. There were residual amounts of ametropia (as given by c_4), varying across subjects, and even across sessions in the same subject. This finding suggests that the defocus that minimizes the RMS wavefront error is not necessarily that for which subjective image quality is best The variation across sessions could also be indicative of some static accommodation varying from session to session. The effect of the residual defocus is a bodily shift of the function up or down the dioptric axis. To examine the differences in the chromatic aberration across sessions and subjects we normalized the data, by adding or subtracting a dioptric amount at each series of data points. We fitted the data to a template function — a third order polynomial, as used by other authors (Howarth, Zhang, Bradley, Still & Thibos, 1988; Charman, 1995) — and calculated the shift that made the function cross zero defocus at a wavelength of 570 nm. Each series of data was then shifted by the amount calculated for the corresponding fitting function. This method for normalizing the data distributes the error across all wavelengths, similar to the method used by Howarth and Bradley (1986). To compute the LCA between 450 and 650 nm we used the fitted polynomial rather than the refractive error for the most extreme wavelengths, to avoid individual errors at these two measurement points. The LCA (between 450

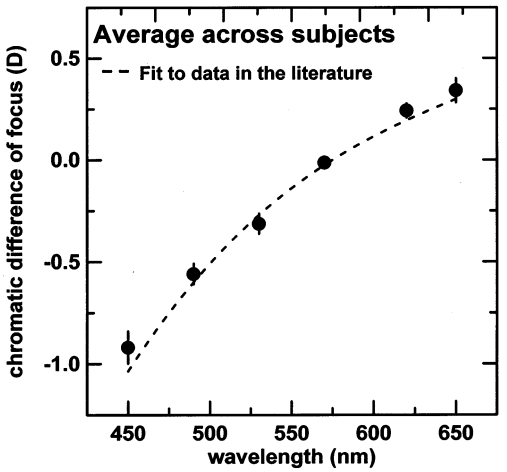

Fig. 2. Longitudinal chromatic aberration (average of three subjects, right eyes). Defocus has been computed from the defocus term (c_4) of the fit to Zernike polynomials of each series of data. The data from different runs and different subjects have been shifted along the dioptric axis, so that the chromatic difference of focus is 0 at 570 nm. Dashed line is a 3rd order polynomial fit to average data from the literature: $20.33 + 0.08534\lambda - 1.1210^{-4}\lambda^2 + 5.93\ 10^{-8}\lambda^3$. Error bars ($\pm 1$ S.D.) indicate intersubject variability.

and 650 nm) for our three subjects was 1.44 ± 0.06 D for EM, 1.20 ± 0.16 D for SM, and 1.13 ± 0.09 D for SB.

3.1.2. Change of monochromatic aberrations with wavelength

Fig. 3a shows the change in astigmatism with wavelength for the three subjects, calculated from coefficients c_3 and c_5 in the Zernike expansion. For the two subjects with higher amounts of astigmatism (EM and SB) there is a significant increase of in astigmatism with wavelength (t-test, $P < 0.01$ and $P < 0.05$, respectively). Fig. 3b shows the variation with wavelength of the dominant aberrations for subject SM (third order terms c_8 and c_9, and spherical aberration, c_{12}, expressed in microns). Whereas variability is too high to define a clear trend for the third order terms, spherical aberration increases significantly with wavelength (t-test, $P < 0.0001$). Fig. 3c shows the wavelength-dependence of the root-mean-square wavefront error (in microns) for the three subjects, leaving out tilt and defocus terms. The RMS wavefront error, which accounts for the deviation of the wavefront with respect to the reference sphere and therefore represents a global description of the system aberrations, increases significantly with wavelength for subjects EM and SB (t-test, $P < 0.005$ and $P < 0.05$, respectively), but not SM.

3.2. Experiment 2

We analyzed the angular spot diagrams (obtained directly from the sets of tilts measured in the spatially resolved refractometer as a function of entry pupil position) for blue and red wavelengths. From the shifts of the spots diagrams for blue with respect to red illumination, we determined the achromatic axis and the transverse chromatic aberration.

3.2.1. Achromatic axis

Fig. 4 shows pupil maps for right and left eyes of subjects SM and SB. These maps represent the calculated angular separation of blue and red spots on the retina as a function of entry pupil position. Each map is the average across six runs (in two separate sessions). Each square represents the corresponding sampled pupil area (which in fact is circular in the measurements). The gray scale value indicates the angular distance between corresponding blue and red spots. The darkest pupil location (minimum angular deviation) corresponds to the achromatic axis. For this pupil location, the subjects also reported that the blue and red retinal spots were superimposed. These maps are equivalent (in 2-dimensions) to the chromatic parallax functions typically reported in the literature with measures only along the horizontal axis (Simonet & Campbell, 1990; Thibos et al., 1990). Table 1 shows the coordinates of the achromatic axis on the pupil plane computed from our 2-D chromatic parallax functions. The coordinates of the achromatic axis have been estimated by a weighted average (using closest neighbors) around the pupil location producing the minimum value of the chromatic parallax function. In the horizontal axis, positive coordinates stand for nasal in the right eye and temporal in the left eye, and negative

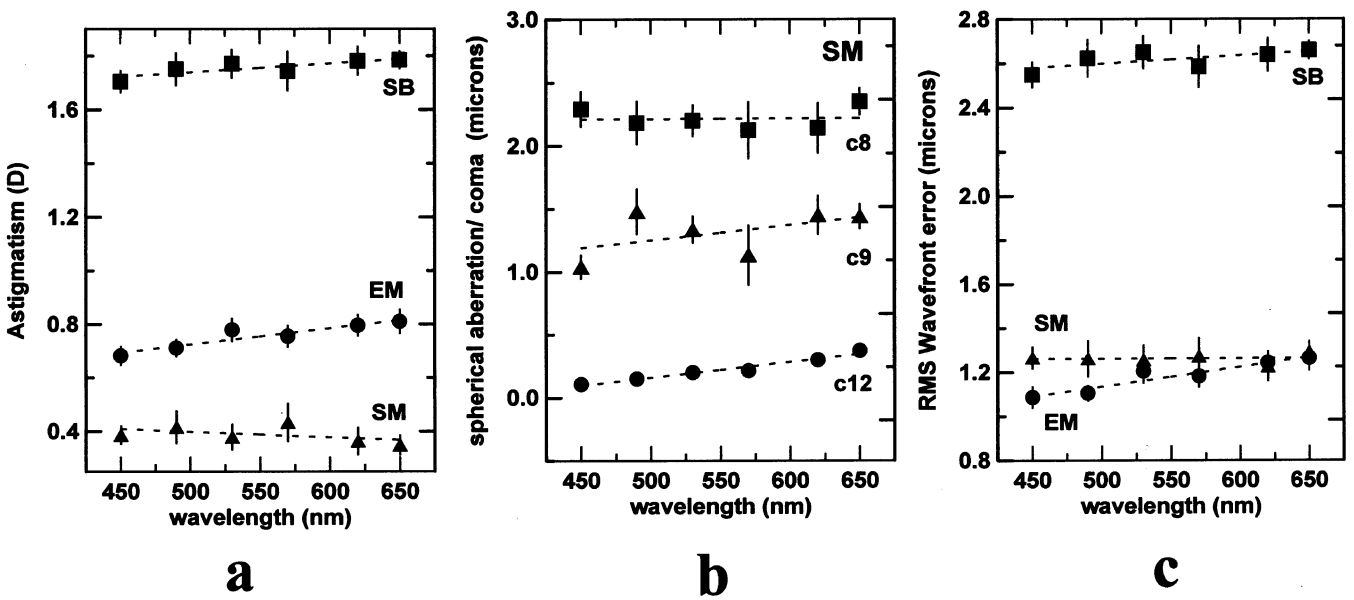

Fig. 3. (a) Change of astigmatism (computed from terms c_3 and c_5 in the Zernike polynomial expansion) as a function of wavelength for all three subjects. (b) Change of 3rd order terms c_8 and c_9 in the Zernike polynomial expansion, and spherical aberration (c_{12}) as a function of wavelength, for subject SM. (c) Change in the root-mean-square wavefront error (expressed in microns) as a function of wavelength, for all three subjects. Symbols are average across runs in four sessions. Error bar represent ± 1 S.E. of the mean.

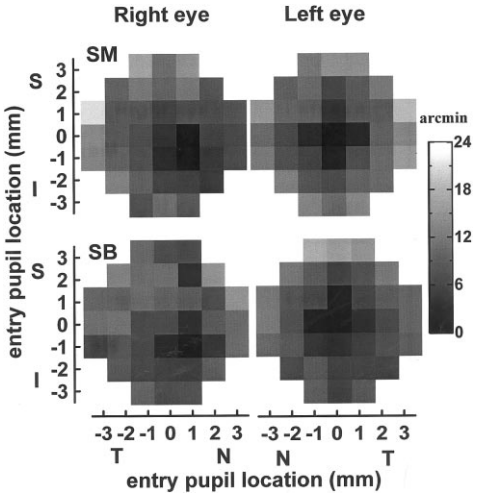

Fig. 4. Pupil maps for left and right eyes of subjects SM and SB showing the achromatic axis. The intensity of each square represents the chromatic parallax [angular deviation in arc min between the blue (473 nm) and red (601 nm) retinal spots] for that entry pupil location. The achromatic axis corresponds to the pupil location for which the chromatic parallax is minimum (darker area in the pupil maps).

coordinates for temporal in the right eye and nasal in the left eye. In the vertical axis, positive coordinates stand for superior and negative for inferior, in both eyes. The achromatic axis is significantly nasal and inferior for these particular subjects' right eyes, and closer to the pupil center in their left eyes.

3.2.2. Optical and perceived TCA

Fig. 5 shows spot diagrams from single sessions for subject SM (right eye) and subject SB (right eye). For each entry pupil location, each spot represents the displacement of the test spot at the oscilloscope with respect to the reference stimulus. Open symbols represent data for blue illumination, and filled symbols data for red illumination. The main aberration for subject SM (right eye) is coma along the vertical axis, and therefore the spot diagrams are elongated in that direction. The main aberration for subject SB (right eye) is astigmatism. The differences in shape between the blue and red spot diagrams are mainly due to blur. The fact that the blue spot diagram is more spread than the red spot diagram indicates that the subjects were undercorrected for green light. The diagram is presented in the same

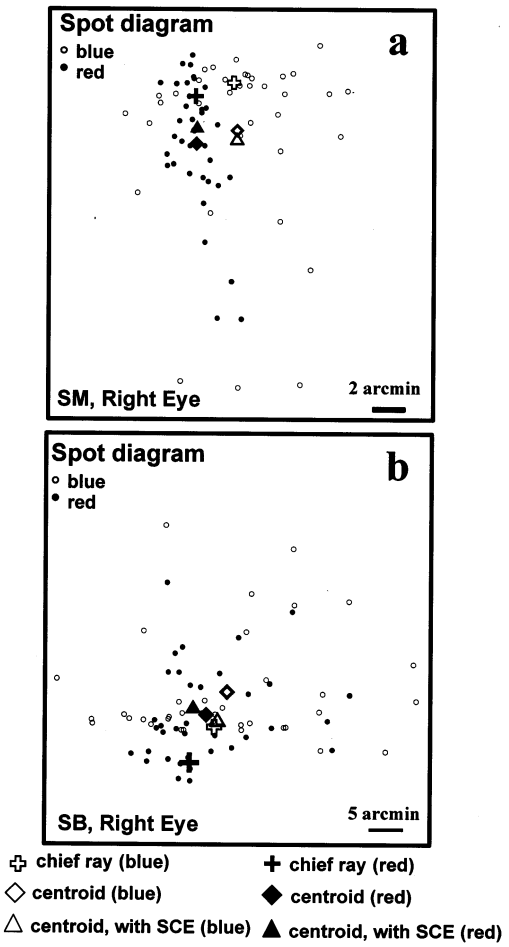

Fig. 5. Spot diagrams for individual sets of data for subject SM, right eye (a) and subject SB, right eye (b). Each circle represents, for each entry pupil, the tilt necessary to null the deviation from a retinal spot with respect to the reference, for blue (open circles) and red (solid circles) illumination. Open and solid crosses represent the chief rays for blue and red respectively, and the distance between the crosses represents the optical TCA. Open and solid diamonds represent the centroids of the spot diagrams for blue and red light, and the open and solid triangles represent the centroids when each spot is weighted by the relative luminous efficiency (SCE) of the corresponding entry pupil location. The distance between centroids represents an estimate of the perceived TCA.

orientation as viewed by the subject. Optical TCA is defined as the displacement of the chief rays with wavelength. The retinal spots corresponding to the centered sample aperture (which defines the chief ray) are marked in Fig. 5 as open and solid crosses, for blue

Table 1
Location of the achromatic axis relative to the geometrical center of the pupil, for left and right eyes of two subjects[a]

Subject	SM (RE)	SM (LE)	SB (RE)	SB (LE)
x coordinate ($\pm$S.D.) (mm)	0.82 ± 0.58	-0.07 ± 0.58	0.92 ± 0.10	-0.30 ± 0.40
y coordinate ($\pm$S.D.) (mm)	-0.31 ± 0.32	-0.08 ± 0.22	-0.88 ± 0.08	0.29 ± 0.44

[a] Results are averages across six runs in two sessions. Positive coordinates in the horizontal direction stand for nasal pupil location in the right eye and temporal in the left eye, and vice-versa for negative coordinates. Positive coordinates in the vertical direction stand for superior pupil locations, and vice-versa for negative coordinates.

and red wavelengths, respectively. The horizontal component of the optical TCA is the difference between horizontal coordinates of the blue and red chief rays, and the vertical component of the optical TCA the difference between vertical coordinates. When asymmetric aberrations are present, the center of the blur of the retinal image is not defined by the chief rays. Perceived TCA is defined as the angular displacement of the centroids of the blue and red retinal images (or for our purposes, of the spot diagrams). The centroids of the spot diagrams shown in Fig. 5 are represented by open and solid diamonds, for blue and red wavelengths, respectively. The difference between horizontal and vertical coordinates of the centroids of the blue and red spot diagrams represent respectively the horizontal and vertical components of the perceived TCA. In addition to aberrations, there is one factor that can modify perceived TCA: the Stiles–Crawford effect (SCE). As a consequence of the SCE effect, certain areas of the pupil are visually more effective than others. The location of the peaks of maximum efficiency is well known for the right and left eyes of our subjects (Burns, He & Marcos, 1998; Marcos & Burns, 1999b). We modeled the SCE as a Gaussian intensity mask at the plane of the pupil, $10^{-\rho[(x-x_0)^2+(y-y_0)^2]}$, with peak locations (x_0, y_0) at $(0, -1)$ mm for both right and left eyes of subject SM, and $(0, -2)$ and $(2, -2)$ mm for right and left eyes of subject SB, respectively (with the same sign convention as for the achromatic axis, Table 1). For reasons explained elsewhere, (Marcos & Burns 1999a; Burns et al., 1998) we took 0.1 mm^{-2} as the shape factor (ρ) of the Gaussian function, for all subjects. The relative brightness of the retinal spots was set proportional to the relative luminous efficiency of the corresponding entry pupil location. The centroids of the spot diagrams modulated by the SCE are represented in Fig. 5 by open and solid triangles, for blue and red wavelengths respectively. Since in these two eyes the SCE peak is displaced toward inferior pupil locations, there is a reversal in the relative location of the vertical component of the blue and red centroids. As in the two previous cases, horizontal and vertical components of the perceived TCA (considering both the aberrations and the SCE) were computed from the coordinates of the centroids for blue and red light. Table 2 shows the horizontal and vertical components of the TCA, for left and right eyes of subjects SM and SB, respectively, for all three cases studied: optical TCA, perceived TCA (taking into account only the aberrations), and perceived TCA (with both aberrations and SCE). We used the following sign convention: for both left and right eyes, the horizontal component of the TCA is positive when the blue spot (or centroid) appears to the subject to the left of the red spot, and vice-versa. This convention matches Thibos et al. (1990) for the left eye, and is the opposite for the right eye. For both eyes, the vertical component of the TCA is positive when the blue spot is below the red spot, and vice-versa.

4. Discussion

4.1. LCA. Effect of aberrations and SCE

The mean LCA of our subjects was 1.26 D (S.D. = 0.16) between 450 and 650 nm. This value is comparable to the average LCA found in the literature, described by a fit to the data compiled by Charman (1995): $0.0853(\lambda_1-\lambda_2)-1.21\cdot10^{-4}(\lambda_1^2-\lambda_2^2)+5.93\cdot10^{-8}(\lambda_1^3-\lambda_2^3)$, which for $\lambda_1=650$ nm and $\lambda_2=450$ nm yields an LCA of 1.33 D. This value is significantly higher than the LCA that we obtained for subjects SM and SB. Recently reported measurements using an objective double-pass technique also provided slightly smaller values of LCA ($\sim$1 D on average between 458 and 632 nm). It has been argued that differences can arise from the different experimental conditions (objective versus subjective, small versus dilated pupil). For example, Thibos et al. (1991) found that estimates of LCA using a best-focusing method (with dilated pupil) were 0.29 D higher, on average, than estimates from a vernier alignment method (in Maxwellian view) on the same subjects. They attributed the discrepancy to the fact that the former estimate of LCA is affected by aberrations, whereas the latter provides a paraxial estimate. The chromatic difference of refraction that we presented in Fig. 2 is based on the defocus term c_4 of the Zernike expansion. It corre-

Table 2
Horizontal and vertical component of the transverse chromatic aberration (TCA), for left and right eyes of two subjects: optical TCA (for the chief rays), perceived TCA I (considering the subject's aberrations) and perceived TCA II (considering the subject's aberrations and their own Stiles–Crawford effect)[a]

Subject	SM (RE)	SM (LE)	SB (RE)	SB (LE)
Horizontal optical TCA ($\pm$S.D.) (arc min)	-3.47 ± 1.03	0.25 ± 0.99	-3.77 ± 1.43	0.22 ± 1.19
Vertical optical TCA ($\pm$S.D.) (arc min)	-2.10 ± 1.84	0.11 ± 1.18	-5.03 ± 1.30	0.40 ± 1.61
Horizontal perceived TCA I ($\pm$S.D.) (arc min)	-3.46 ± 0.55	-0.10 ± 0.93	-1.95 ± 1.43	-0.17 ± 0.52
Vertical perceived TCA I ($\pm$S.D.) (arc min)	-1.66 ± 0.96	-0.66 ± 0.52	-2.71 ± 1.70	-0.61 ± 1.15
Horizontal perceived TCA II ($\pm$S.D.) (arc min)	-3.29 ± 0.58	0.22 ± 1.49	-2.77 ± 1.15	3.73 ± 0.47
Vertical perceived TCA II ($\pm$S.D.) (arc min)	2.16 ± 1.51	2.32 ± 0.71	1.99 ± 0.92	3.74 ± 1.16

[a] Results are averages across six runs in two sessions. Positive coordinates mean that the subject perceived the blue to the left of the red or blue on top of the red for horizontal and vertical directions respectively, and vice-versa for negative coordinates.

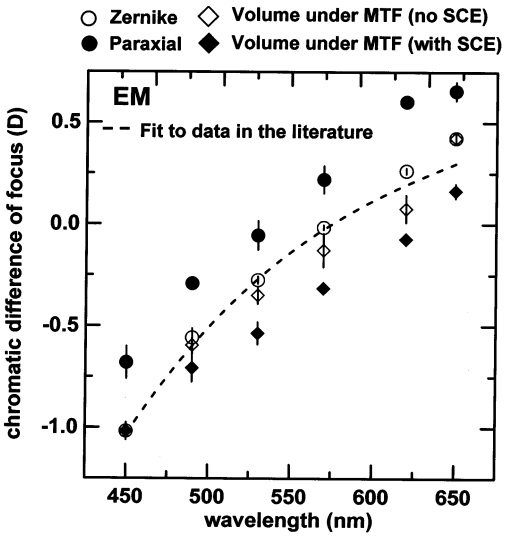

Fig. 6. Chromatic difference of focus for subject EM, using different definitions for plane of focus. Open circles stand for defocus from the term c_4 in the Zernike polynomial expansion. Solid circles stand for defocus computed from all quadratic terms in the Zernike polynomial expansion (c_4, c_{12} and c_{24}) and represents the chromatic difference between paraxial planes of focus. Diamonds represent the refraction that produces a maximum in the through-focus image quality (computed from the volume under the MTF), not considering the SCE (open) or considering the SCE (solid). All data have been shifted along the dioptric axis so that the chromatic difference of Zernike defocus is zero at 570 nm. Paraxial defocus (equivalent to refraction for a diffraction-limited pupil) shows a hyperopic shift with respect to Zernike defocus (refraction for a big pupil). For this subject, including the SCE produces a myopic shift in the function. Symbols are averages across four sessions. Error bars are ± 1 S.E. of the mean. Dashed line is a 3rd order polynomial fit to average data from the literature, as in Fig. 2.

sponds to the refractive correction that provides minimum RMS wavefront error with a large pupil. The paraxial focus can be computed by combining all the terms in the Zernike polynomial expansion that contain quadratic terms (c_4 and c_{12} and c_{24} in our expansion), and it should be equivalent to the refraction for a diffraction-limited pupil. We have computed paraxial chromatic difference of focus for our subjects. As in previously reported studies (Howarth & Bradley, 1986), all our subjects show a systematic shift of the paraxial function toward hypermetropic corrections (0.26 D for EM, 0.24 D for SM and 0.85 D for SB), but the overall change of wavelength remains very similar. We did not find any systematic trend for the variation of LCA between the two methods, and the differences were within the experimental error. Fig. 6 shows the chromatic difference of focus, for subject EM, using different criteria: (1) defocus term in the Zernike expansion (open circles); (2) paraxial defocus, from the quadratic terms in the Zernike expansion (solid circles); (3) defocus that maximizes the volume under the MTF, ignoring the SCE (open diamonds); (4) defocus that maximizes the volume under the MTF, considering the SCE (solid diamonds). For cases (3) and (4) we calculated series of modulation transfer (MTFs) for a series of defocus (at 0.15 D steps), simulated by adding positive and negative amounts of defocus to term c_4 in the Zernike expansion. We then computed the volume under the MTFs (truncated at 115 c deg^{-1} to avoid contributions of spatial frequencies irrelevant for the visual system) as a function of defocus and obtained the defocus that maximized the volume, for each wavelength. For case (4) we considered the Stiles–Crawford function of this subject, with peak at (0, 0.4) mm and $\rho = 0.1$ mm^{-2}. The chromatic difference of paraxial defocus shows the mentioned hypermetropic shift. The function obtained using the criteria of maximum volume under the MTF (not considering the SCE) is very similar to the one obtained from the Zernike defocus term: the LCA obtained from these two different criteria is not significantly different (1.432 ± 0.006 D, using the volume under the MTF, versus 1.442 ± 0.006 D, using the Zernike defocus term). However, for this particular subject, we found significant differences when the SCE was introduced. The function obtained from the volume under the MTF considering SCE shows a myopic shift (especially for longer wavelengths), despite the smaller effective pupil size produced by the SCE. Particular aberrations in combination with the SCE may produce important asymmetries of the through focus image quality, possible generating a displacement of the focus that produces a maximum in the through-focus function (Burns et al., 1998; Zhang, Ye, Bradley & Thibos, 1999; Atchison, Joblin & Smith, 1998). For this subject, we found a slightly smaller value of LCA when the SCE effect was included (1.176 ± 0.008 D).

4.2. Achromatic axis and TCA. Comparison with other studies

Previous studies have primarily addressed only the horizontal component of the TCA, and provided only the horizontal coordinate of the achromatic axis. We have estimated both horizontal and vertical components. However, although the number of sample apertures in the present study was higher than in previous studies (37 versus 13 in Simonet & Campbell, 1990, and in Thibos et al., 1990), our resolution was lower, mainly because in our method the sample apertures were more separated (1 mm in our study, and 0.2–0.64 mm in previous studies). As a result, the accuracy of the estimation of the shift of the achromatic axis with respect to the pupil center (SD of 0.08–0.58 mm in our study) was lower than in the mentioned studies (SD of 0.02–0.20 mm). We obtained also a lower precision in the estimation of the foveal TCA (SD of 0.52–1.84 arc min in our study versus SD of 0.17–0.88 arc min in the earlier studies). Our previous work on the reliability of the data collected with the spatially resolved refrac-

tometer (He et al., 1998a), yielded standard deviations of 0.93 arc min across repeated angular alignments, roughly the same order as the standard deviations found in the present study. Part of the increase in the variability may be due to the use of a larger sample pupil (1 mm in our study, versus 0.5–0.6 mm in the mentioned studies). The larger pupils may increase the difficulty of the alignment task, particularly for eccentric entry locations (where even a 1 mm pupil is not diffraction-limited). Finally, our measurement was the difference of two alignments (blue spot to the reference, and red spot to the reference), whereas in a conventional vernier alignment task only one alignment is required (blue line with respect to the red line).

Nevertheless, the accuracy was sufficient to support the following findings. As others, we found that the achromatic axis was displaced nasally from the center of the pupil in all the eyes tested. However, in two eyes (SM, right eye and SB, right eye) this shift is much larger (0.82 and 0.92 mm, for SM and SB, respectively), than in previous studies (-0.08 to 0.51 mm) — see Table 1. In these two eyes we also found significant displacements of the achromatic axis toward inferior pupil locations, particularly for subject SB. Finally, we also found an asymmetry in the location of the achromatic axis between eyes of the same subject. The achromatic axis in the left eyes of these two subjects is close to the center of the pupil (see Table 1 and Fig. 4).

The displacements of the achromatic axis with respect to the center of the pupil are reflected in the values of the optical TCA (see Table 2). The horizontal component of the optical TCA for subject SB's right eye is at least 2.4 times larger than the highest value found in studies by Simonet and Campbell (1990) and Thibos et al. (1990) even though our spectral range using the magenta filter is 1.48 times smaller. However, the horizontal component of the optical TCAs in the left eyes is consistent with previously published data. To our knowledge, there are no experimental data of the vertical component of the TCA in the literature. Theoretical eye models (Bennet & Rabbetts, 1984; Thibos, 1987) predict that the vertical component should be approximately half the horizontal component, which is not what was measured in subject SB's right eye (where the vertical component is 1.33 times the horizontal component). Those predictions are based on the displacement of the fovea with respect to the optical axis (angle $\alpha = 5°$ on average in the horizontal meridian and 2.5° on average in the vertical meridian according to Tscherning, 1924), and in the position of the pupil behind the corneal surface. Although there is evidence of anatomical differences of these parameters across individuals, it seems unlikely that the large amounts of TCA found in our subjects arises from an unusually large angle α. Another suggested explanation for the differences of TCA between eyes are shifts of the position of the pupil center with dilation. Typical values of ± 0.2 mm in the horizontal direction (Walsh, 1988) are not sufficient to explain our results. Our results suggest that simple eye models are not adequate to explain TCA in all eyes, since misalignment of the optical components may play an important role in the amount of TCA present. Curiously, there seems to be some correlation between optical quality and amount of TCA in the four eyes measured. These two subjects, who had an asymmetry in the amount of optical TCA between right and left eyes, also had a strong asymmetry in the optical quality between right and left eyes. From measurements presented elsewhere (Marcos & Burns, 1999b) RMSs of the wavefront aberration are 1.8 and 0.4 μm for the right and left eyes of subject SM, respectively, and 1.9 and 1.1 μm for right and left eye of subject SB, respectively ($\lambda = 530$ nm). It is likely that misalignment of the lens and the cornea and nonuniformities of the optical elements, which degrade optical quality in those eyes, are also the source of their high TCA values.

4.3. Optical and perceived TCA. Effect of aberrations and SCE

It has been argued that measurements of the TCA using a small centered pupil (optical TCA) can be different from those measuring perceived TCA with dilated pupils (Simonet & Campbell, 1990). In fact, changes in the magnitude and/or direction of the TCA with pupil have been suggested as the reason for changes in the magnitude of chromostereopsis (Vos, 1960; Sundet, 1972;Ye et al., 1992; Rynders, 1994; Winn, Bradley, Strang, McGraw & Thibos, 1995): If the blue image is perceived to the left of the red image in the right eye, and to the right in the left eye, the blue object will appear to be closer than the red object. Some studies (Vos, 1960; Sundet, 1972; Ye et al., 1992) found that chromostereopsis changed (in general decreased, and sometimes even changed sign) as the pupil diameter increased, although this does not appear to be a general result. Several authors have suggested that the effect could be due to changes in the optical TCA as the pupil center shifts with pupil dilation (Kishto, 1965). Another hypothesis suggests that optical aberrations and the SCE peak location interact to alter perceived TCA (Vos, 1960). Our data provide direct information on the effect of aberrations and SCE on perceived TCA. The results appear in Table 2. We observe that the effects vary strongly across individuals, and between eyes in the same individual, and that the effect of the SCE on the amount of TCA varies across eyes. Since for all our cases the SCE is displaced vertically with respect to the pupil center, we found that the SCE had a large effect on the vertical component of the TCA, causing it to reverse. We may expect a change in

subject's SB chromostereopsis, since the horizontal component of the TCA changes significantly with pupil size for the left eye. We only observed a decrease in the magnitude of the TCA for subject SB's right eye with increasing pupil size, especially in the vertical component, because both the vertical coordinates of the achromatic axis and the SCE peak lie in the inferior pupil (-0.93 and -2 mm, respectively). In fact, the location of the SCE peak seems to critically affect the perceived TCA: we have calculated that the perceived TCA for this subject would be reduced to practically zero if the coordinates of the SCE peak were (1.35, -1.4) mm, i.e. much closer to the achromatic axis. Therefore, in eyes where the SCE peak lies close to the achromatic axis (as in Vos, 1960's experiments, where all four eyes had nasal SCE), TCA is reduced for larger pupils. That could also be the case in the eyes tested by Ye et al. (1992), who also found smaller TCA for large pupils, especially under photopic conditions.

4.4. Variation of optical quality with wavelength

LCA and TCA are important for viewing stimuli in polychromatic light. When we are dealing with monochromatic illumination, TCA is not present, and LCA can be corrected with appropriate lenses. However, for many psychophysical experiments or when trying to image retinal structures, we may consider (ignoring other issues) which wavelength should be used to achieve maximum resolution. Fig. 3c shows that the RMS (in microns) of the wavefront aberration increases significantly with wavelength in two eyes. Fig. 7 shows the variation with wavelength of different parameters commonly used to describe optical quality, for subject EM. Solid symbols in Fig. 7a show the increase with wavelength of RMS, as in Fig. 3c. Open symbols in Fig. 7a represent the same RMS, but expressed in wavelengths. This function, which represents the phase of the pupil function, and is more meaningful optically, decreases with wavelength (i.e. the effect of the aberrations decreases with wavelength). Optical quality is usually expressed in terms of the volume under the MTF, or volume under the MTF relative to a diffraction-limited system (strehl ratio). The higher the volume (or the strehl ratio) the better the optical quality. Solid symbols show the increase of strehl ratio with wavelength: i.e. the higher the wavelength the closer the eye is to a perfect optical instrument. However, the actual volume under the MTF is higher (higher resolution) for shorter wavelengths (open circles). Given that frequencies higher than ~ 100 c deg^{-1} are not relevant to the visual system (Williams, 1985), we have also computed the volume under the MTF, clipping out modulations at frequencies higher than ~ 100 c deg^{-1}. This operation has a much larger effect for shorter-wavelengths (which have higher cut-off frequencies). As a consequence, the optical quality computed for the truncated MTF (open triangles) decreases with wavelength more slowly than when all frequencies are considered (by a factor of two between the most extreme wavelengths, as opposed to a factor of four). Therefore, Fig. 7 shows that different optical quality metrics emphasize different aspects of the data. RMS wavefront error reflects the change in the phase of the pupil function, but does not include diffraction effects which appear in the modulus of the pupil function. Strehl ratio is a relative measure, and compares optical quality to the perfect lens, for the same pupil size and wavelength. Volume under the MTF is an absolute measure, independent of pupil size and diameter. However, modulation at high spatial frequencies must be ignored if we want to account for what it is relevant to the visual system.

4.5. Optical quality in polychromatic light

There have been several attempts in the literature to characterize the optical quality of the human eye in

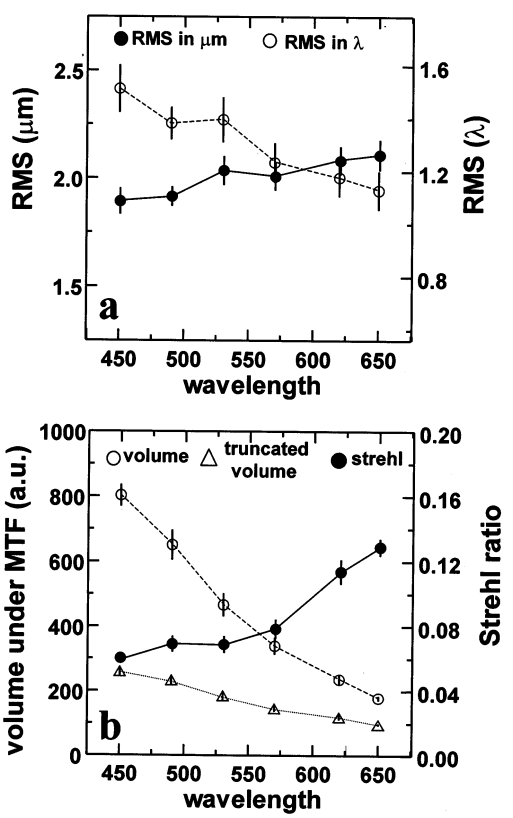

Fig. 7. Analysis of the optical quality as a function of wavelength, for subject EM. (a) RMS in microns (solid circles) and in wavelengths (open circles). (b) Volume under the MTF (open circles), volume under the MTF, ignoring frequencies beyond ~ 100 c deg^{-1} (open triangles), and volume under the MTF normalized by the volume of the diffraction-limited eye, i.e. strehl ratio (solid circles). Symbols are averages across four sessions. Error bars are ± 1 S.E. of the mean. Pupil radius was 3.66 mm,[1] and the SCE was not taken into account.

polychromatic light. Several studies evaluated the influence of LCA and TCA on visual performance using psychophysical tasks (Hartridge, 1947; Campbell & Gubish, 1967). Thibos, 1987 and Thibos et al. 1991 computed the influence of lateral chromatic aberration on the optical quality of the human eye, based on simple eye models. Van Meeteren, 1974 derived a general MTF of the human eye using typical values for low-order aberrations. The current data include both LCA and TCA, as well as wavefront aberration across wavelengths in individual subjects. We used these data to compute the polychromatic optical quality in the eye with largest TCA (SB, right eye), and evaluated the influence of several factors (SCE, TCA, LCA). We computed the PSFs in polychromatic light by superimposing PSFs for different wavelengths, calculated from the corresponding wavefront aberrations. To avoid artifacts produced by our sparse sampling of the spectrum (six wavelengths) we interpolated the sets of Zernike coefficients, and obtained wavefront aberrations at wavelength steps of 5 nm, from which we computed PSFs as a function of wavelength. We used a fit to the previously described third order polynomial to interpolate the defocus term, and a cubic spline method to interpolate the rest of the coefficients. The PSFs were weighted by the photopic spectral sensitivity curve for the CIE standard observer (Wyszecki & Stiles, 1982) and added with lateral displacements, linearly interpolated from the value of TCA for subject SB (Table 2). We simulated the PSF in polychromatic light (including both TCA and LCA), and in polychromatic light, corrected for LCA, TCA and both LCA and TCA. Correction of the LCA (which can be achieved experimentally by placing an achromatizing lens in front of the eye, Howarth & Bradley, 1986; Bradley, Zhang & Thibos, 1991; Zhang, Thibos & Bradley, 1997) was simulated by setting the defocus term (c_4) to zero for all wavelengths. Correction of the TCA (which can be achieved by appropriate prisms) was simulated by setting TCA to zero. Finally, we evaluated the effect of the SCE on polychromatic PSFs. Fig. 8 shows computed MTFs (MTF radial profiles versus spatial frequency)

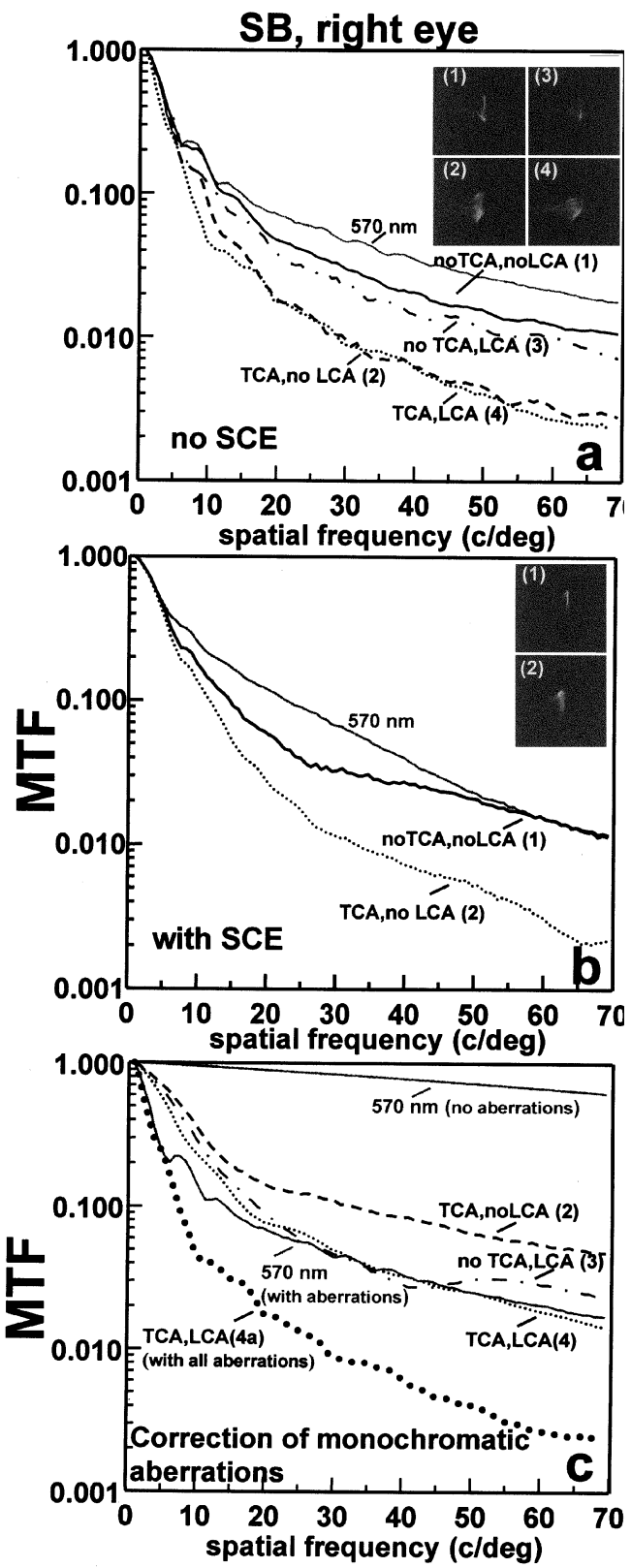

Fig. 8.

Fig. 8. Optical quality in polychromatic light for SB, right eye (3.66 mm pupil radius). LCA and aberrations as a function of wavelength were obtained from Experiment 1 and TCA from Experiment 2. Data were interpolated to compute PSFs at 5 nm wavelength intervals (between 450 and 650 nm), which were weighted by spectral sensitivity curve for the CIE standard observer, and added with a displacement computed from the measured TCA. The illuminant was an equal energy white. The inset images represent the PSFs for the cases shown in the figure. The curves represent radial profiles of the MTF for the corresponding PSFs. (a) Without including the SCE; (b) including the SCE for this subject; (c) assuming compensation for monochromatic aberrations at 570 nm, also including monochromatic MTF with aberrations (lower solid curve) and MTF with monochromatic and chromatic aberrations (thick dotted curve). No TCA, no LCA means that both TCA and LCA have been set to 0 in the calculations; no TCA, LCA means that TCA has been set to 0; TCA, no LCA means that LCA has been set to 0; TCA, LCA means that both TCA and LCA have been included in the calculations.

and PSFs (inset images) without SCE (a) and with SCE (b), considering the monochromatic and polychromatic aberrations, and location of Stiles–Crawford peak of subject SB (right eye). The MTF in polychromatic light, correcting both TCA and LCA (solid black line) is only slightly worse than for 570 nm (solid gray line). The MTF for polychromatic light considering only the effect of LCA is represented by the dotted-dashed lines. The MTF for polychromatic light including TCA, with and without correction for LCA are represented by dashed and dotted lines, respectively. The inset images show the corresponding PSFs. For this subject, correction of TCA would significantly improve contrast modulation (by a factor of 2.5 for 30 c deg^{-1}). This could explain the increase of resolution in Snellen optotypes observed by Hartridge (1947) after compensation of TCA, even if the LCA was not corrected. Also, the MTF including TCA but compensated for LCA is very similar to the MTF including both LCA and TCA, which could explain Campbell and Gubish's (1967) observation that visual resolution did not increase by correcting LCA with achromatizing lenses. TCA highly reduces contrast for all spatial frequencies, but especially for medium and high frequencies. For example, for 30 c deg^{-1} TCA would reduce the contrast by a factor of 0.32. This attenuation is larger than the contrast attenuation of 0.95 predicted by Simonet and Campbell (1990) based on Thibos (1987) calculations (in fact, we obtain a very similar factor, 0.93, when we use Simonet & Campbell's mean TCA). Fig. 8b shows the effect of the SCE. The SCE increases the MTF, but the degradation caused by the TCA remains. However, the PSF in polychromatic light clearly shows the mentioned reversal of the centroid of the PSF, when the SCE is included. Insets (1) and (2) in Fig. 8b, to be compared to insets (1) and (2), respectively in Fig. 8a, illustrate the centroid reversal induced by the SCE.

Finally, we have calculated the impact of chromatic aberrations in an eye corrected for monochromatic aberrations for a single wavelength. Liang, Williams and Miller (1997) using adaptive optics techniques, showed that the monochromatic MTF can be improved, by compensating part of the monochromatic aberrations. Whereas this correction is undoubtedly useful to image fine structures in the retina — where typically monochromatic light is used — it is not clear if there would be the visual benefit of compensation of static monochromatic aberrations for seeing the real world in polychromatic light (Yoon, Cox & Williams, 1999). Fig. 8c shows the effect of polychromatic aberrations in subject SB's right eye, assuming a perfect correction of aberrations at 570 nm. The solid lines show respectively the MTF for 570 nm with monochromatic aberrations, and after ideal compensation for all monochromatic aberrations (i.e. a diffraction-limited eye). Dashed, dotted-dashed, and dotted-dotted lines represent the cases of polychromatic illumination assuming that LCA has been compensated, TCA has been compensated, or both TCA and LCA are present, respectively, assuming that the monochromatic aberrations have been corrected. Thick dotted lines represent the MTF when all aberrations (monochromatic and chromatic) are present. TCA alone (along with some residual contribution of aberrations not completely compensated for wavelengths different than 570 nm) is responsible for an attenuation of the modulation of 0.13 at 30 c deg^{-1} in an eye ideally corrected for 570 nm. TCA and LCA impose an attenuation of 0.06 at 30 c deg^{-1}. While the polychromatic MTF after monochromatic aberrations corrections is still higher than the monochromatic MTF with no correction, for middle and high spatial frequencies this difference is reduced. At 30 c deg^{-1}, the monochromatic, non-corrected MTF is 0.046, whereas the polychromatic MTF corrected for monochromatic aberrations is 0.049. From Fig. 8, it is clear that the relative impact of chromatic aberrations is much higher for a perfect eye (i.e. compensated for monochromatic aberrations) than for an aberrated eye. Also, when chromatic aberrations are present, the relative improvement of optical quality resulting from correcting monochromatic aberrations is less than for the monochromatic case. For example, at 30 c deg^{-1}, the monochromatic MTF (570 nm) improves by a factor of 18 when monochromatic aberrations are totally compensated (ratio of the two gray curves in Fig. 8c), whereas the polychromatic MTF (including TCA and LCA) only improves by a factor of 5.4 (ratio of two dotted line curves in Fig. 8c). This finding indicates that chromatic aberrations (both TCA and LCA) should not be ignored when evaluating the visual benefit of a compensation of monochromatic aberrations. It is also important to note that these relations depend critically on the spatial frequency of interest, and on the aberration structure of the particular eye. We have shown results for the worst of the eyes in this study.

5. Conclusions

Using a spatially resolved refractometer, we have measured the wavefront aberration at different wavelengths. We conclude that:

1. LCA in the 450–650 nm range is 1.26 D on average. Differences across subjects, and from results obtained from the literature are small. LCA is not significantly influenced by pupil size, although the Stiles–Crawford effect (SCE) may slightly affect the LCA in particular subjects.
2. Location of the achromatic axis and the amount and direction of the horizontal and vertical components of the TCA vary highly across subjects, and can even vary between eyes in the same individual.

3. Aberrations and SCE modify the amount and direction of the TCA. SCE does not necessarily reduce the impact of TCA.
4. Aberrations tend to increase with wavelength, and the RMS (in microns) increases with wavelength in two of our three subjects. Different metrics for optical quality emphasize different aspects, and optical quality increases or decreases with wavelength depending on the metric used. For instance, while the volume under the MTF decreases with wavelength, the strehl ratio increases.
5. In aberrated eyes, TCA can degrade the MTF as much as the LCA. Correcting the TCA (leaving the effect of LCA) can improve the MTF more than correcting the LCA while leaving the TCA uncorrected.
6. The impact of chromatic aberrations on diffraction-limited eyes (i.e. compensated for monochromatic aberrations) is large. At middle and high spatial frequencies, the degradation imposed by chromatic aberrations to an eye corrected for monochromatic aberrations (using polychromatic light) can be as large as the degradation imposed by monochromatic aberrations (using monochromatic light).

Acknowledgements

We would like to thank Doug Goger for calibrations of the spectrum of the oscilloscope phosphor and spectral transmission of the filters. Supported by Public Health grants EYO4395, and Department of Energy Center of Excellent Grant DE-FG-02-91ER61229 and Comisión Interministerial de Ciencia y Tecnología (Spain) under grant TIC98-0925-C02-01. S. Marcos was funded by Human Frontier Science Program Postdoctoral Fellowship LT-542/97. E. Moreno-Barriuso was funded by a Ministerio de Educación y Cultura (Spain) Predoctoral Fellowship.

References

Artal, P., Marcos, S., Iglesias, I., & Green, D. G. (1996). Optical modulation transfer function and contrast sensitivity with decentered small pupils. *Vision Research*, *6*, 3575–3586.

Atchinson, D. A., Woods, R. L., & Bradley, A. (1998). Predicting the effects of optical defocus on human contrast sensitivity. *Journal of the Optical Society of America A*, *15*, 2449–2456.

Atchison, D. A., Joblin, A., & Smith, G. (1998). Influence of Stiles–Crawford apodization on spatial visual performance. *Journal of the Optical Society of America A*, *15*, 2545–2551.

Bedford, R. E., & Wyszecki, G. (1957). Axial chromatic aberration of the human eye. *Journal of the Optical Society of America*, *47*, 564–565.

Bennet, A. G., & Rabbetts, R. B. (1984). *Clinical visual optics*. London: Butterworths.

Bradley, A., Zhang, X. X., & Thibos, L. N. (1991). Achromatizing the human eye. *Optometry and Vision Science*, *68*, 608–616.

Burns, S. A., He, J. C., & Marcos, S. (1998). The influence of cone directionality on optical image quality. *Investigative Opthalmology and Visual Science* (*Suppl.*), *39*, 203.

Campbell, F. W., & Gubish, R. W. (1967). The effect if chromatic aberration on visual acuity. *Journal of Physiology* (*London*), *186*, 558–578.

Charman, W. N., & Jennings, J. A. M. (1976a). Objective measurements of the longitudinal chromatic aberration of the human eye. *Vision Research*, *16*, 999–1005.

Charman, W. N., & Jennings, J. A. M. (1976b). The optical quality of the monochromatic retinal image as a function of focus. *British Journal of Physiological Optics*, *31*, 119–134.

Charman, W. N. (1995). The optics of the eye. In M. Bass, *Handbook of optics* (2nd ed.). New York: McGraw-Hill.

Emsley, H. H. (1952). *Visual optics* (5th ed.). London: Hatton Press.

Hartridge, H. (1947). The visual perception of fine detail. *Philosophical Transactions of the Royal Society of London*, *29*, 311–338.

He, J. C., Marcos, S., Webb, R. H., & Burns, S. B. (1998a). Measurement of the wave-front aberration using a fast psychophysical procedure. *Journal of the Optical Society of America A*, *15*, 2449–2456.

He, J. C., Burns, S. A., & Marcos, S. (1998b). The change in the aberration of the human eye with accommodation. *Investigative Opthalmology and Visual Science* (*Suppl.*), *39*, 396.

Howarth, P. A., & Bradley, A. (1986). The longitudinal chromatic aberration of the human eye, and its correction. *Vision Research*, *26*, 361–366.

Howarth, P. A., Zhang, X., Bradley, A., Still, D. L., & Thibos, L. N. (1988). Does the chromatic aberration of the eye change with age? *Journal of the Optical Society of America A*, *5*, 2087–2092.

Howland, H. C., & Howland, B. (1977). A subjective method for the measurement of the monochromatic aberrations of the eye. *Journal of the Optical Society of America*, *67*, 1508–1518.

Ivanoff, A. (1953). *Les aberrations de l'oeil*. Paris: Editions de la Revue D'Optique Théorique et Instrumentale.

Jenkins, T. C. A. (1963). Aberrations of the eye and their effects on vision — part II. *British Journal of Physiological Optics*, *20*, 161–201.

Kishto, B. N. (1965). The colour stereoscopic effect. *Vision Research*, *5*, 313–329.

Le Grand, Y. (1956). *Optique physiologique. L'espace visuel*, vol. III. Paris: Éditions de la Revue d'Optique.

Liang, J., Grimm, B., Goetz, S., & Bille, J. F. (1994). Objective measurements of wave aberrations of the human eye with the use of a Hartmann-Shack wave-front sensor. *Journal of the Optical Society of America A*, *11*, 1949–1957.

Liang, J, Williams, D. R., & Miller, D. T. (1997). Supernormal vision and high-resolution retinal imaging through adaptive optics. *Journal of the Optical Society of America A*, *14*, 2884–2892.

Mahajan, V. N. (1994). Zernike circle polynomials and optical aberrations of systems with circular pupil. *Applied Optics*, *33*, 8121–8124.

Malacara, D. (1992). *Optical shop testing* (p. 465). New York: Wiley.

Marcos, S., & Burns, S. A. (1999a). Cone spacing and waveguide properties from cone directionality measurements. *Journal of the Optical Society of America A*, *16*, 995–1004.

Marcos, S., & Burns, S. A. (1999b). Cone directionality and wave-front aberration: are they symmetric between eyes? *Investigative Opthalmology and Visual Science* (*Suppl.*), *40*, 365.

Marcos, S., Moreno, E., & Navarro, R. (1999). The depth of field of the human eye from objective and subjective measurements. *Vision Research*, *39*, 2039–2049.

Navarro, R., Moreno, E., & Dorronsoro, C. (1998). Monochromatic aberrations and point-spread functions of the human eye across visual field. *Journal of the Optical Society of America A*, *15*, 2522–2529.

Navarro, R., & Losada, M. A. (1997). Aberrations and relative efficiency of light pencils in the living human eye. *Optometry and Visual Science*, *74*, 540–547.

Noll, R. J. (1976). Zernike polynomials and atmospheric turbulence. *Journal of the Optical Society of America*, *66*, 207–211.

Ogboso, Y. U., & Bedell, H. E. (1987). Magnitude of lateral chromatic aberration across the retina of the human eye. *Journal of the Optical Society of America A*, *4*, 1666–1672.

Rynders, M. C. (1994). *The Stiles–Crawford effect and an experimental determination of its impact on vision*. Ph.D. dissertation. Indiana University, Bloomington.

Rynders, M. C., Navarro, R., & Losada, M. A. (1998). Objective measurement of the off-axis longitudinal chromatic aberration in the human eye. *Vision Research*, *38*, 513–522.

Simonet, P., & Campbell, M. C. W. (1990). The optical transverse chromatic aberration on the fovea of the human eye. *Vision Research*, *30*, 187–206.

Sundet, J. M. (1972). The effect of pupil size variations on the colour stereoscopic phenomenon. *Vision Research*, *12*, 1027–1032.

Thibos, L. N., Bradley, A., Still, D. L., Zhang, X., & Howarth, P. A. (1990). Theory and measurement of the ocular chromatic aberration. *Vision Research*, *30*, 33–49.

Thibos, L. N., Bradley, A., & Zhang, X. (1991). Effect of ocular chromatic aberration on monocular visual performance. *Optometry and Vision Science*, *68*, 599–607.

Thibos, L. N. (1987). Calculation of the influence of lateral chromatic aberration on image quality across the visual field. *Journal of the Optical Society of America A*, *4*, 1673–1680.

Tscherning, M. (1924). *Physiological optics*. Philadelphia: Keystone.

Van Meeteren, A. (1974). Calculations of the optical modulation transfer function of the human eye for white light. *Optica Acta*, *21*, 395–412.

Vos, J. J. (1960). Some new aspects of colour stereoscopy. *Journal of the Optical Society of America*, *50*, 785–790.

Wald, G., & Griffin, D. R. (1947). The change in refractive power of the human eye in dim and bright light. *Journal of the Optical Society of America*, *37*, 321–366.

Walsh, G. (1988). The effect of mydriasis on the pupillary centration of the human eye. *Ophthalmic and Physiological Optics*, *8*, 178–182.

Webb, R. H., Penney, C. M., & Thompson, K. P. (1992). Measurement of the ocular wavefront distortion with a spatially resolved refractormeter. *Applied Optics*, *31*, 3678–3686.

Williams, D. R. (1985). Aliasing in human foveal vision. *Vision Research*, *25*, 195–205.

Winn, B., Bradley, A., Strang, N. C., McGraw, P. V., & Thibos, L. N. (1995). Reversals of the colour-depth illusion explained by ocular chromatic aberration. *Vision Research*, *35*, 2675–2684.

Wyszecki, G., & Stiles, W. S. (1982). *Color science — concepts and methods, quantitative data and formulae*. New York: Wiley.

Ye, M., Bradley, A., Thibos, L. N., & Zhang, X. (1992). The effect of pupil size on chromostereopsis and chromatic diplopia: interaction between the Stiles–Crawford effect and chromatic aberrations. *Vision Research*, *32*, 2121–2128.

Yoon, G, Cox, I, & Williams, D. R. (1999). The visual benefit of the static correction of the monochromatic wave aberration. *Investigative Opthalmology and Visual Science* (*Suppl.*), *40*, 40.

Zhang, X., Thibos, L. N., & Bradley, A. (1997). Wavelength-dependent magnification and polychromatic image quality in eyes corrected for longitudinal aberration. *Optometry and Visual Science*, *74*, 563–569.

Zhang, X., Ye, M., Bradley, A., & Thibos, L. N. (1999). Apodization by the Stiles–Crawford Effect moderates the visual impact of retinal image defocus. *Journal of the Optical Society of America A*, *16*, 812–820.